Fuel Processing Technology 275 (2025) 108259

Contents lists available at ScienceDirect

Fuel Processing Technology

journal homepage: www.elsevier.com/locate/fuproc

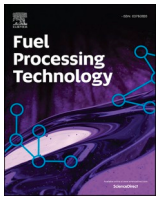

Valorization of municipal solid waste from Marocco towards hydrogen, methanol, or electricity: An experimental and process simulation study

Cesare Freda [a], Aristide Giuliano [a], Antonio Villone [a], Giacinto Cornacchia [a], Enrico Catizzone [b,*]

[a] ENEA – Italian Agency for New Technologies, Department of Energetic Technologies, Trisaia Research Centre, I-75026 Rotondella, Italy
[b] Chemical Engineering Catalysis and Sustainable Processes Laboratory (CECaSP_Lab, Department of Environmental Engineering, University of Calabria, via P. Bucci, 87036 Rende (CS), Italy

ARTICLE INFO

Keywords:
Municipal solid waste
Process simulation
Gasification
Pyrolysis

ABSTRACT

Worldwide population growth and improvements in living standards are leading to a significant increase in municipal solid waste production, particularly in developing countries. In these regions, a well-established waste management strategy is often lacking, and alternatives to illegal landfills must be explored. Pyrolysis is a technology that can be used for the valorization of MSW to produce high-value products. However, several aspects require further elucidation for industrial application. This study aims to assess the valorization of unsorted MSW from Morocco, focusing on the production of methanol, hydrogen, or electrical power. To this end, both pyrolysis of MSW and gasification of the residual char were experimentally investigated to generate raw syngas. Computer-aided process simulations were then conducted to evaluate the technical and environmental aspects of converting the resulting syngas mixtures into the desired products: methanol, pure hydrogen, or electricity.

1. Introduction

The heterogeneous mix of refuse generated daily by urban residents, known as municipal solid waste (MSW), encompasses a range of materials. This includes organic remnants like food scraps, along with paper, plastics, metal containers, textiles, glass, and other discards. The precise makeup of MSW varies considerably across different municipalities and is subject to seasonal and temporal fluctuations [1,2]. Establishing an effective system for MSW collection is the foundational step towards recovering or recycling valuable resources, thus fostering a circular economy model.

However, many developing nations face substantial challenges in managing MSW, leading to significant adverse socioeconomic and environmental effects [3]. Morocco, a developing country with around 32 million people, with 51 % residing in urban areas and an annual population growth rate of 2.85 %. The combination of rapid population increase and growing urbanization is driving a marked escalation in MSW production, causing serious environmental concerns, particularly in cities. Morocco's MSW output is on a steady rise, currently reaching 9 million tons annually. Waste handling in the country is hampered by inadequate collection practices, largely delegated to the private sector, and the proliferation of unregulated landfills. These illegal sites are estimated to process roughly half of the total MSW generated. Such mismanagement has detrimental impacts on economic progress, tourism, and overall living standards [4–8].

To mitigate the problems associated with uncontrolled and hazardous landfilling, it's vital to explore and implement efficient MSW management strategies. In this context, the National Municipal Waste Plan (PNDM) was initiated in 2008, with the goal of regulating all urban landfills in Morocco by 2015. This objective was not achieved, leading to an extension of the deadline to 2020. However, the current situation remains far from the desired outcomes. Furthermore, the PNDM outlines the following objectives: achieving 100 % MSW collection by 2030; attaining a 20 % recycling rate of produced MSW by 2022; improving waste sorting and recovery; and creating at least 70,000 jobs within the waste management sector [9]. This plan draws inspiration from the sustainability principles of the circular economy, which, within the European Union, is manifested through "Waste hierarchy actions," providing a tiered framework for waste management. This is often referred to as the "4-R hierarchy," which includes Reduce, Reuse, Recycle, and Recovery [10]. Various techniques, including combustion, pyrolysis, gasification, anaerobic digestion, and landfill gas extraction, are being utilized to extract valuable resources (e.g., energy, chemicals, or fuels) from MSW [11–14].

* Corresponding author.
E-mail address: enrico.catizzone@unical.it (E. Catizzone).

https://doi.org/10.1016/j.fuproc.2025.108259
Received 31 March 2025; Received in revised form 27 May 2025; Accepted 4 June 2025
Available online 11 June 2025

Pyrolysis, a well-established method traditionally used for producing charcoal from biomass, involves heating solid feedstock in an oxygen-free environment to yield solid, liquid, and gaseous fuels [15]. More recently, relatively uniform waste materials such as tires, automotive shredder residue, and plastics have been employed as feedstock for industrial-scale pyrolysis. However, the significantly more diverse composition and size of MSW compared to these materials makes its pyrolysis more complex, especially when collection is limited, as is common in developing countries. Makarichi et al., using Harare as a case study, assessed the composition, moisture content, thermochemical properties, and energy content of MSW in a typical African city [16]. Their findings suggested that the quality of MSW is comparable to that in regions outside Africa where waste-to-energy initiatives have been successful. He et al. examined the effect of temperature on the pyrolysis of Chinese MSW using calcined dolomite as a catalyst in a bench-scale fixed-bed reactor [17]. Raising the temperature from 750 to 900 °C resulted in increased MSW conversion to product gas, with notable increases in H_2 and CO content, reaching 36 and 30 mol%, respectively. Char and tar yields decreased, while dry gas yield and carbon conversion increased, with a minimal impact on the syngas's lower heating value (LHV) of approximately 13 MJ/Nm^3. Calcined dolomite enhanced gas yield and reduced oil and char yields compared to non-catalytic processes [17]. Li et al. conducted separate pyrolysis of various solid wastes (paper, cardboard, plastics including PVC and PE, rubber, plant materials, wood, and orange peel) in an externally heated rotary kiln [18]. They observed that higher temperatures promoted the breakdown of larger molecules, and the gas's heating values peaked at different temperatures for each waste type. Moisture content was identified as a critical factor influencing gas yields. Luo et al. (2010) performed lab-scale fixed-bed reactor pyrolysis tests on MSW from Wuhan, China, to evaluate the influence of particle size (up to 20 mm) and bed temperatures on product yield and composition [19]. They discovered that smaller particles yielded more gaseous products and less tar and char, though this effect diminished with increasing temperature. Smaller MSW particles also resulted in higher H2 and CO yields, improving gas quality and yield.

The charcoal produced from MSW pyrolysis still constitutes a waste product, requiring further valorization techniques to minimize its volume. In this context, the remaining organic material can be subjected to gasification. Gasification transforms solid carbonaceous material into a fuel gas, primarily composed of carbon monoxide, hydrogen, and methane. This process involves the reaction of the carbonaceous material at temperatures between 700 and 900 °C with a controlled, sub-stoichiometric amount of oxidant (air/oxygen or steam), leaving behind an inorganic residue (ash). Numerous studies have investigated the gasification of biomass-derived char, evaluating the impact of various parameters (e.g., temperature, pressure, catalyst presence, gasifying agent type, char textural properties) on gas yield and quality [20–24].

This study aims to evaluate the potential for valorising uncollected MSW from Agadir, Morocco, using thermal treatment methods. Specifically, MSW was initially pyrolyzed at varying temperatures (350–550 °C), and the resulting charcoal was subsequently gasified in air to maximize total gas yield and minimize residual solids.

The originality of this research stems from the scarcity of existing literature on fuel recovery from MSW in Morocco or other developing countries through thermal treatments. It is essential to recognize that feedstock type, temperature, and other variables significantly affect both pyrolysis and gasification processes. Therefore, experimental investigations are crucial to gain new insights into the potential of these thermal processes for uncollected MSW valorization.

Furthermore, a techno-environmental assessment, utilizing computer-assisted simulations, was conducted to assess the valorization of the obtained raw syngas into fuels (e.g., hydrogen), chemicals (e.g., methanol), or electricity. This work aims to promote a waste-to-chemicals strategy, even for challenging, uncollected MSW. Globally, the novelty of the work is related to both experimental and simulation approach and results. A common problem for developing countries like Morocco is indeed huge population and poor resources, such as electricity. Therefore, an investigation about the conversion of uncollected MSW into valuable products for the country, also going beyond the electricity, such as methanol or hydrogen, represents one of the most significant approaches for viewing MSW as a resource, also contributing to the sustainability and technological advances. In developing countries like Morocco, agriculture is a fundamental industry, therefore the production of hydrogen could be also considered as potential interest for the production of ammonia or e-chemicals like methanol [25]. As reported below, the thermochemical conversion to syngas was experimentally investigated by using uncollected MSW with no significant pre-treatment and adopting a dual-stage concept consisting in pyrolysis followed by gasification of residual char with a rotary kiln. This approach allows to propose a promising technology for the valorization of the selected feedstock, and simulation demonstrates the environmental benefits in terms of carbon dioxide emission savings. Studies on the same topic are usually focused on the valorisation of refused derived fuel (RDF), whose production requires several steps, such as shredding, magnetic stirring, grinding, screening and sometimes pelletizing [26–29]. In the present study, the uncollected MSW was used as received with no pre-treatment directly converted in the pyrolysis unit. At the best of the authors' knowledge, for the first time a facile route for thermochemical valorisation of uncollected MSW has been experimental demonstrated, and the further valorisation of the gas obtained by both pyrolysis and gasification step assessed by comparing three different scenarios, i.e. production of hydrogen, methanol or electricity, useful for future advances in process development.

2. Experimental

2.1. Feedstock supply

Approximately 33 kg of municipal solid waste (MSW) from Agadir, Morocco, were utilized in this study. The waste was collected from open areas, representing a significant and representative sample of unsorted municipal waste from two distinct neighbourhoods: Tikiouine and Elfarah. To create an analytical sample of roughly 5 kg, the collected waste underwent a quartering process. The as-received sample exhibited a slight malodor, likely due to fermentation, and was subsequently stored in a fume hood for stabilization. Visual inspection identified the following material classes: plastics, paper, organics, fines, inerts, metals, and textiles. A manual separation of these classes was performed, and the gravimetric amount of each class was determined using an analytical laboratory balance to quantify the waste's material composition.

Ultimate analysis of the sample was conducted using a Perkin Elmer Series II 2400 CHN/O elemental analyzer, following ISO 16948. Specifically, sulfur, fluorine, chlorine, phosphorus, and bromine were quantified by bubbling the exhaust gas from the calorimetric bomb through an alkaline buffer solution of Na_2CO_3 and NaHCO3, where they were absorbed as anions (Cl^-, SO_4^{2-}, F^-, PO_4^{3-}, Br^-). The anion concentrations were then measured using High Performance Ion Chromatography (Dionex DX 300). The metal concentrations of the inert-free MSW were determined as follows: the sample was mineralized with aqua regia, hydrogen peroxide, and hydrofluoric acid. The resulting mixture, filtered through 0.45 μm cellulose paper, was analyzed using an Agilent ICP-EOS 720. The metals measured included Al, Co, Cr, Cu, Mn, Mo, Ni, Pb, Ti, Tl, V, Zn, Ca, K, Mg, Na, Si, and Fe.

Moisture content was determined according to UNI EN 15414, ash content according to UNI EN 14775, and fixed carbon and volatile matter were estimated using UNI EN 15148. The heating value was measured using an IKA C4000 Bomb Calorimeter, following UNI EN 14918.

2.2. Pyrolysis and gasification tests

Pyrolysis tests were carried out in a semi-batch plant with a fixed bed reactor hosted in a modified Lenton tube furnace of 5 kW, equipped with a temperature controller. The schematic diagram of the experimental rig is showed in Fig. 1.

The experimental setup for the pyrolysis test includes a nitrogen gas cylinder (1) equipped with a pressure reducer (2) and a flow meter controller (3). A furnace (5) encloses an alumina reaction tube (7.6 cm internal diameter, 100 cm in length), within which a cylindrical and perforated sample holder (4) is positioned. This holder has a diameter of 7 cm and a height of 50 cm. To aid in the removal of pyrolysis vapors by the carrier gas and prevent the loss of char, the reactor holder feature perforations with a diameter of 1 mm. The process temperature is controlled by a Temperature Indicator and Controller (TIC) (6), which receives its input from a thermocouple located inside the furnace. A second thermocouple (7) is placed directly within the sample holder to monitor the temperature of the sample as it undergoes treatment. The generated pyrolysis gas is then passed through three bubbler flasks (8) containing a 1 M sodium hydroxide alkali solution, which is kept at −20 °C using a laboratory-prepared ice bath with sodium chloride to dissolve organic vapors and water. Most of the vapors are condensed in the first flask, and the second and the third is used to further clean the gas to be sent for analysis. The calculated oil yield refers to the total oil collected by weighting the flasks before and after the test. Following this, the gas stream flows through a biomass biological filter (9), is quantified using a gas volumetric meter, and is analyzed every three minutes by an Agilent 3000 A gas chromatograph to determine the volumetric composition of hydrogen, carbon monoxide, carbon dioxide, methane, and other light hydrocarbons.

In a typical test, about 430 g of MSW inert free were put in the sample holder. Once, that the sample holder was assembled inside of the furnace, 1 l/min of nitrogen fluxed the semi batch plant to create an inert atmosphere. The furnace heated the reactor at 10 °C/min up to the set temperature that was measured by a thermocouple placed inside the feedstock. The test run for about 120 min, and during this time the temperature was monitored obtaining an average process temperature value with a variation of ±10 °C during the test. At the end of the test, the electrical heating was switched off. When the furnace reached environmental temperature, the residual char was recovered and weighted for the mass balance and stored for the chemical-physical analyses, i.e. proximate analysis, elemental analysis and LHV determination. The three bubbler flasks were weighted to determine the bio-oil fraction.

Gasification of the char obtained from pyrolysis (pyro-char), was performed in a bench scale rotary kiln plant as schematized in Fig. 2 [30]. The rig is very similar to that used for pyrolysis, but a different thermochemical unit was adopted as described below.

The bench-scale rotary kiln reactor was produced by Lenton (PTF 16/75/610 model) having an internal alumina pipe with an inner diameter of 78 mm and length of 1.2 m, equipped with a feeding hopper with a capacity of 5 lt. The char was continuously fed to the alumina reactor by means of a water-cooled screw-driver device. The furnace was heated by three independent electrical resistances. Three thermocouples measured the temperature of each heated zone along the wall of the reactor.

The residual char was continuously discharged into a reservoir at the outlet of the reactor. The raw gas flow throughout a plenum chamber and successively, it crossed the cleaning system to condense tar, particulate and water. The cleaning system was composed of three bubblers of 1 lt. Each of them was filled with 500 ml of ethanol and kept in a bath of water-ice at temperature of 0 °C (element 8 in Fig. 2). The gas crossed a biological filter composed of a fixed bed of dry biomass (element 9 in Fig. 2).

Downstream of the cleaning system, a volumetric gas meter measured the dry gas flow. A portion of the gas was then analyzed using the same micro gas chromatography system employed for the pyrolysis tests. The reactor operated under a slight positive pressure (5–10 mbar), maintained by the liquid depth in the bubblers. The following procedure was implemented for the gasification tests. In a typical test, 110 g/h of pyro-char was gasified with 60 standard liters per hour (STD l/h) of air, with the kiln maintained at a 3° slope and a rotation speed of 5 rpm. This resulted in an equivalence ratio of approximately 0.5. The oven was heated at a rate of 5 °C/min until reaching the target temperature of 800 °C. Subsequently, the char feed and air flow were initiated. During the test, particulate matter, tar, and water were removed using ethanol-filled bubblers. At the test's conclusion, the ethanol solutions were collected and weighed. Approximately 200 mL of the mixture was filtered through a 10 μm pore diameter fiberglass filter. The filter's weight difference was recorded to determine the particulate content. This procedure for particulate determination is more efficient than standard isokinetic sampling, particularly when dealing with relatively low gas volumes, as in this study. Generally, it yields results comparable to isokinetic sampling. The water content was measured by Karl Fischer titration of the ethanol solution. The gravimetric tar content was determined according to CEN15439. The filtered ethanol solution was prepared for gas chromatography–mass spectrometry (GC–MS) analysis. Chromatographic analyses were performed using an Agilent Technology 5975 B GC–MS system, equipped with an HP-5MS cross-linked 5 % PhMe-siloxane 30 m × 0.25 mm × 0.25 μm film thickness column. Helium (99.9999 %v) was used as the carrier gas. For tar molecule quantification and identification, a 6-level calibration curve and multi-standard solutions were employed. Tar sampling was conducted with slight modifications from CEN/TS 15439, due to logistical constraints.

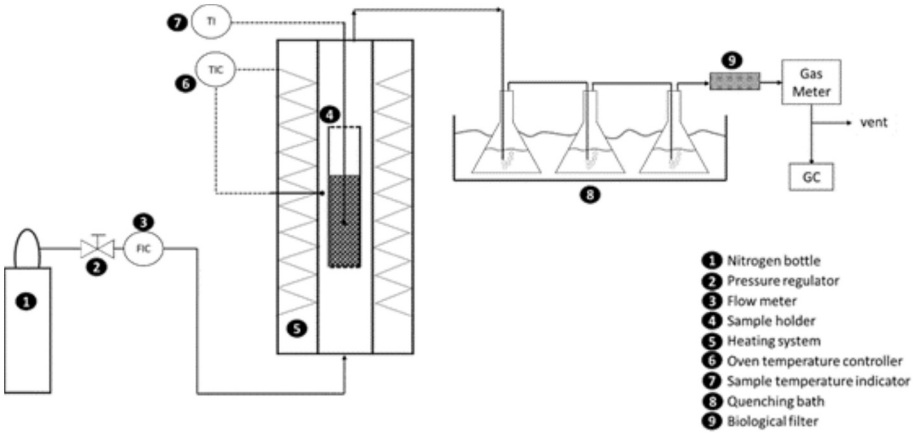

Fig. 1. Scheme of experimental rig for pyrolysis tests.

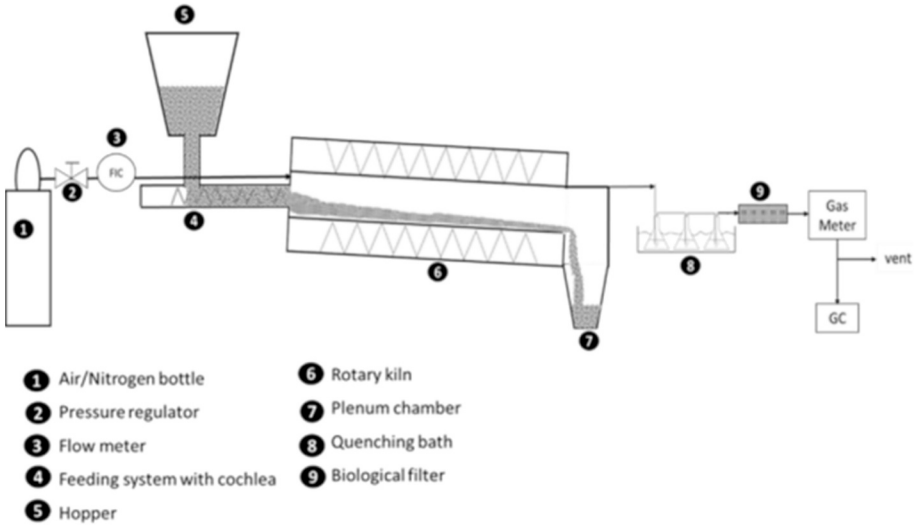

Fig. 2. Scheme of experimental rig for gasification tests.

The test duration was approximately 2 h. To terminate the test, the screw feeder inverter, kiln rotation, electrical heating, and air flow were shut down. The plant was purged with nitrogen inert gas. Once the reactor cooled to room temperature, the residual char was collected from the reservoir. The gas produced during gasification was analyzed with the same procedure used for pyrolysis tests. During the gasification test no slagging was observed, and a low tar content detected as described later, indicating a promising suitability of the proposed technology for the selected feedstock.

2.3. Flowsheets and process simulation

Process design tools [31] were utilized to identify all process streams in plants designed to valorize pyrogas and syngas derived from MSW pyrolysis. As previously mentioned, both pyrogas and syngas obtained from gasification can be employed to generate energy or high-value products, including chemicals and fuels such as methanol, dimethyl ether, Fischer-Tropsch hydrocarbons, and hydrogen [32–37]. Therefore, the gas streams produced during pyrolysis at 341 °C and gasification are assumed to be mixed, cleaned and used for downstream processing. A flowrate of 100′000 t/y of uncollected MSW is adopted for simulation. This section assesses three distinct scenarios for gas stream valorization. Specifically, this paper considers the production of electricity (Case-EL), methanol (Case-MeOH), and pure hydrogen (Case-H2). For this purpose, the process simulation software CHEMCAD was employed. The Redlich-Kwong-Soave thermodynamic equation of state was selected to simulate high-pressure systems, while the NRTL-RK equation was used for distillation columns and flash separation units.

In particular, the liquid stream from pyrolysis was considered capable of sustaining the endothermic pyrolysis process. By burning the high mass flow rate of bio-oil, the pyrolysis was maintained at the same temperature as the experimental tests.

For Case-EL the gas streams produced from both pyrolysis of MSW and gasification of residual char were mixed to be sent as fuel to an internal combustion engine for the production of electricity, according to the scheme reported in Fig. 3.

After mixing the gases are considered free of particulate or tars. An engine [38] is considered for the combustion of syngas after mixing with air. Air flowrate was optimized in order to maximize the electricity production. The simulation software can model the coupling of gas compression, combustion, and turbine operation using an ideal isentropic hypothesis as a conventional endothermic engine burning gases. By optimizing the discharge pressure and flame temperature through adjustments in air mass flow rate, the best gas turbine efficiency was

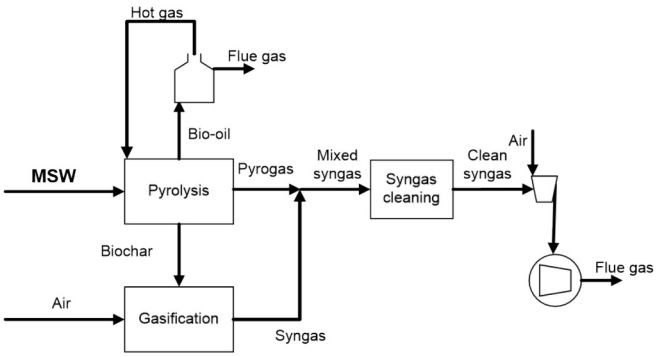

Fig. 3. Flowsheet of valorization of MSW for producing of electrical power.

identified.

Methanol is one of the most important compounds of the chemical industry, with an annual production of about 40 million tons and an annual market increase rate of 4 %. Currently, methanol is mainly produced from syngas obtained via steam reforming of fossil carbon sources, mainly natural gas and coal. In particular, a higher CO_2 amount is emitted from coal-based plants. Aiming to reduce both CO_2 emission and fossil source supply, alternative carbon sources may be considered in the light of a sustainable energy economy. In this concern, the syngas obtained from gasification of biomass, residuals and waste may be considered as raw streams to obtain methanol.

At this regard, for Case MeOH considered in this work, the clean syngas (pyrogas+syngas after gas treatment) was sent to a (i) WGS section to convert CO into CO_2 and hydrogen, followed by (ii) a carbon capture section by Selexol process to obtain a $(H_2\text{-}CO_2)/(CO + CO_2)$ ration equal to 2. After that, (iii) a methanol production and purification section were considered for producing high pure methanol. A flowsheet scheme is reported in Fig. 4. Herewith, such sections are briefly detailed.

The high-pressure capture of carbon dioxide and the production of methanol or pure hydrogen require the conversion of carbon monoxide and steam into CO_2 and H_2, coming with the clean syngas stream, by means of the Water Gas Shift (WGS) reaction.

The WGS reaction is carried out in two steps, namely High Temperature Shift (HTS) and Low Temperature Shift (LTS) [12]. The main operating parameter of this process is the H_2O/CO molar ratio (Steam to Carbon, SC). The clean gas is mixed with a superheated steam (1 bar, 400 °C). The adopted feed ratio was chosen to obtain a H_2O/CO molar ratio (Steam to Carbon, SC) equal to 2.5. The two fixed bed reactors

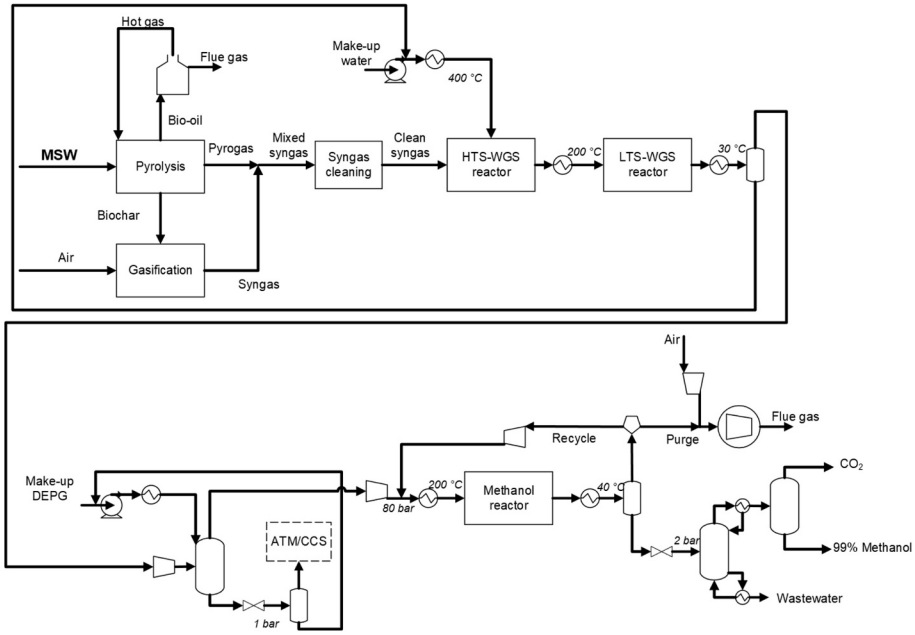

Fig. 4. Flowsheet of valorization of MSW for producing methanol.

modeled as equilibrium reactors. The pressure drop in the sequence of the two catalytic fixed bed, was assumed of about 2 bar [39].

The methanol synthesis was simulated using an equilibrium approach, consistent with the exothermic reaction approximation for well-studied methanol synthesis. WGS was used to convert CO contained in syngas into CO_2 and H_2, increasing the CO_2 molar fraction and consequently its partial pressure, to facilitate CO_2 absorption by the Selexol process. The final upgrading to pure H_2 must be achieved via Pressure Swing Adsorption PSA, which removes residual CO_2 and CO. Figs. 4 and 5 illustrate the CO_2 capture process using Selexol®. All energy requirements and capture rates were evaluated and optimized. However, the localization of the storage was not considered, in line with the hypothesis of a simple storage of compressed CO_2 at up to 110 bars.

For the case of the traditional process sketched in Fig. 4, the section for CO_2 separation with the Selexol® technology is located after the WGS reactor and, thus, the inlet stream to the section is a clean syngas enriched in H_2 and CO_2 [39]. Differently, for the case of the innovative process sketched in Fig. 3, the Selexol® section is located after the partial H_2 separation by membrane and, thus, the inlet stream is richer in CO_2.

The separation of CO_2 from the enriched syngas stream is carried out by absorption in the proprietary solvent Selexol®, a mixture of dimethyl ethers of polyethylene glycol ($CH_3O(C_2H_4O)nCH_3$), where "n" is between 3 and 9, in a packed tower with 75 mm IMTP® packing of Koch-Glitsch®.

The Selexol® solvent is compressed and sent to the top of the tower 30 °C. Solvent regeneration is carried out downstream the absorption tower to separate carbon dioxide and to recycle the solvent. However, a

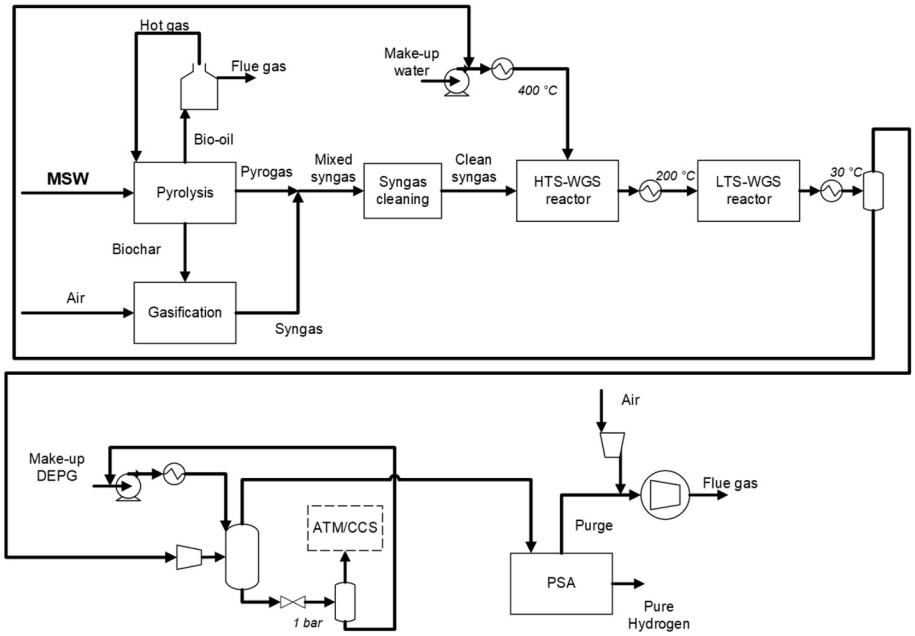

Fig. 5. Flowsheet of valorization of MSW for producing hydrogen.

small make-up stream is necessary to replace the solvent entrained in the gaseous stream leaving the packed tower. In particular, the regeneration is performed by lowering the pressure in two stages by means of two expansion valves up to 1 bar.

A flash is used to recover the CO_2 from the solvent. The regenerated solvent is mixed with the make-up stream and recycled back to the absorption tower after proper recompression. Low pressure captured CO_2 is considered emitted for the comparison with case of CO_2 captured and stored at 110 bar. In this last case, the recovered CO_2, which has the required purity (at least 98.5 % by weight), is compressed up to 110 bars by a compressor train, formed by three compressors with intercooling by two heat exchangers, for storage conditions.

Reactor for methanol production was modeled as equilibrium unit by considering formation of methanol via hydrogenation of both CO and CO_2. Water gas shift is included as well.

In addition, unwanted side reactions, such as formation of methane, dimethyl ether, higher alcohols, and other oxygenates, e.g. aldehydes, also can take place. In this paper, WGS was considered as side reaction only. Because methanol formation is an exothermic reaction, methanol synthesis is favoured at low temperature, from a thermodynamic point of view. Nevertheless, kinetic aspects have to be considered. For these reasons, methanol synthesis is usually carried out in the temperature range 250–280 °C by using Cu-ZnO/alumina as catalyst. Inlet stream to methanol reactor is mixed with recycle stream (unreacted syngas), heated up to 200 °C and fed to the methanol synthesis adiabatic reactor. A pressure drop equal to 2 bar was assumed along the reactor [12]. Concerning operating pressure, a 80 bar pressure is considered to favor thermodynamics.

As mentioned before, crude methanol needs to be purified from water and impurities. As WGS is considered only, dissolved gases, such as CO_2, CO and H_2, are the mainly impurities that need to remove from methanol stream. At this purpose, the output stream of methanol synthesis reactor was cooled down at 40 °C and the light gases are separated in a flash-phase-separator. A part of the separated gases was recompressed at 80 bar and recycled to the reactor, while the rest was used as fuel for electricity production. The liquid streams, mainly consists of methanol and water, was expanded in a throttling valve at 2 bar and distilled to produce a methanol rich stream which was further purified in a flash phase-separator to obtain a 99 % methanol.

Hydrogen is considered one promising alternative to fossil fuel, especially because its combustion release energy with water as “by-product”. The great interest towards hydrogen as energy carrier is because it can be generated from a wide variety of renewable or non-renewable primary energy sources. Actually, most of the hydrogen is produced by fossil source-based processes, such as (i) steam reforming of methane, (ii) partial oxidation, (iii) auto-thermal reforming and (iv) dry-reforming [12]. Although most of the hydrogen is actually produced from fossil sources (about 95 %), the utilization of renewables, such as biomass, has received considerable attention in recent years. In particular, biomass gasification may be used as a suitable technology to produce syngas and then hydrogen. In fact, the syngas produced from gasification may be converted into a H2-rich stream by water gas shift reaction [40,41].

At this regard, for Case-H2 considered in this work, the clean syngas streams obtained from both pyrolysis and gasification unit were mixed and, after WGS and Selexol carbon capture process, they were sent to the Pressure Swing Adsorption (PSA) for purifying and then producing 99.99 % hydrogen. A scheme of the simulated process is reported in Fig. 5.

The PSA is a batch process consisting of a sequence of four steps: adsorption, depressurization, purge and pressurization [39]. The adsorption pressure and the purge ratio (P/F) are the operating variables of the PSA process. In our case, the operating pressure was fixed equal to the output pressure from the absorption column. In the Adsorption step the adsorption time is a fraction of the breakthrough time of N_2. In the Purge step the pure hydrogen, obtained during the adsorption step, is sent, in countercurrent, through the bed in order to allow further desorption of previously adsorbed species, N_2 and CO primary. Purge gas is sent to the engine to produce electricity. A lower content of H_2 in the purge corresponds to higher pure hydrogen recovery and lower power output. Purge gas and air are mixed before compression and engine section. Engine pressure was optimized to maximize the electricity production.

2.4. Environmental impact analysis

For each process case, a final environmental impact analysis was conducted in terms of total CO_2-equivalent emissions [42], using the values provided in Table 1. In particular, a negative CO_2-equivalent emission value is associated with Municipal Solid Waste (MSW), considering the CO_2 emitted from the landfill during MSW disposal [43]. The estimated environmental savings for the bio-methanol production plants investigated were compared to the methanol production from fossil sources, which is 1643 kgCO2eq/tMeOH when coal is used as feedstock [44]. The environmental savings for pure hydrogen production were based on the case of a mixed-source feedstock [45]. Finally, the electricity production savings were assumed to be equal to those of the fossil-based energy production system [43]. The use of process water in the Water-Gas Shift (WGS) reaction has a relatively low environmental impact, even when considering the detoxification and demineralization processes.

The main direct CO_2 emission points are:

- Flue gases of the combustion of the bio-oil [46];
- Flue gases of the combustion of purge gas or of syngas for the case EL;
- CO2 derived by carbon capture section for the cases without CO2 compression and storage.

Table 1 then shows the CO_{2eq} savings (indicated with a minus sign) and emissions (indicated with a plus sign) used to calculate the impacts of the proposed process. In particular, landfill avoidance and the substitution of fossil-based methanol or hydrogen were the main parameters of the analysis.

3. Results

3.1. Waste characterization

A merceological analysis was carried out by considering the following classes: plastics, paper, organics, fines, inserts, metals and textile.

The inerts and metals merceological class is composed of waste such as coarse metal pieces, glasses, tins etc. having dimension above 30 mm. It is reasonable to assume that they could be easily removed from the native waste before to feed it to the thermal plant. Therefore, the chemical physical analysis was executed after having ruled out manually the inerts and metals class. Anyway, to have a complete frame on the waste composition along its cycle, the experimental values of the analysis measured on the MSW inerts and metals free (here onwards MSW inert free), were mathematically rearranged to derive the values of the chemical physical analysis on the as received “unsorted” MSW.

Table 1
CO_2 equivalent emission parameters.

Process item	CO_2 equivalent emission
MSW ($kgCO_2eq/t$) [43]	−1′821
Electricity ($kgCO_{2eq}$/MWhe) [43]	−600
MeOH ($kgCO_{2eq}$/t) [44]	−1′643
Pure hydrogen ($kgCO_{2eq}$/t) [45]	−12′000
Process water ($kgCO_{2eq}$/t) [43]	6.5
Biochar residual ($kgCO_{2eq}$/t) [43]	1′821

The results reported in Table 2 show that the received waste has a highly complex and heterogeneous nature, primarily consisting of organics and paper. Its particle size distribution ranges from centimeters to millimeters. It is noteworthy that materials from all the classes are brown in color due to contamination with sand and ground powder. It is reasonable to assume that these materials were collected from piles of garbage left in the streets for a prolonged period, leading to soil contamination. The sand and ground powder mainly consist of inert materials, which reduce the energy density of the waste and increase the energy demand of thermal processes. This factor is crucial for assessing the technical and economic feasibility of the process. Therefore, it is strongly recommended to implement a waste collection system that prevents contamination with soil. The fines fraction, with a millimetric particle size distribution and a dark brown color, cannot be easily classified into specific material classes. In other words, it cannot be distinguished as plastics, textiles, paper, organics, or inerts, and thus, was classified as fines. After separating the waste into material classes, each class was milled using a Retch laboratory hammer mill. Fluffy powders were obtained, and a representative sample of the MSW fluffy powder was recomposed according to the relative material classes from Table 2, excluding the inert and metal classes. The images of the as-received municipal solid waste and the milled, inert-free samples are shown in Fig. 6.

Proximate and elemental analysis, heating value were carried out on the fluffly powder of MSW inert free. The results are shown in Table 3.

The proximate analysis reveals the presence of a significant amount of both moisture and ash. Nevertheless, after drying and the removal of inerts and metals fraction, the waste showed an interesting low heating value of 17.8 MJ/kg, which is comparable with the heating value of lignocellulosic biomass. As matter of fact, the merceological analysis of Table 2 shows a cellulosic-like fraction, sum of papers and organics of about 60–70 wt%. The heating value together with a volatile content of 71.6 %, set the waste as interesting feedstock for thermal processes addressed to secondary fuels production. Results in terms of metal concentration are reported in Table 4.

The most abundant metals in inert-free MSW are in the following order: Fe, Ca, Si, Na, and K. Alkali and earth alkali metals (Na, K, Ca, Mg) are known to be highly reactive, especially when present as oxides, hydroxides, chlorides, sulfides, and sulfates. The high ash content and their elemental composition must be carefully considered, as they can lead to undesirable thermal phenomena such as softening, melting, and fly ash formation, particularly in processes where high-temperature spots can be reached in the reactor [47,48]. Specifically, MSW-derived fly ash consists of particles that are generally spherical in shape and range in size from a few micrometers to several hundred micrometers. These particles, due to their Cu(II) and Fe(III) content, can catalyze the chemical synthesis of harmful dioxins in the temperature range of 200 to 450 °C [49].

3.2. Pyrolysis tests

Pyrolysis tests were conducted at four different temperatures (350, 450, 500, and 550 °C). The temperature was increased from room temperature to the desired level. During the heating phase, pyrolysis vapors began to form at approximately 200 °C, likely due to moisture release and the initial devolatilization of the waste.

Table 2
Merceological analysis of investigated waste.

Fraction	Distribution (wt%)
Organics	42.3
Papers	24.1
Textiles	5.9
Plastics	6.8
Fines	6.5
Inerts and metals	14.4

Fig. 7 illustrates the distribution of pyrolysis products—pyro-char, pyro-oil, and pyro-gas—as a function of pyrolysis temperature. The char yield slightly decreased with increasing temperature, dropping from approximately 38 % at 350 °C to 30 % at 550 °C. This trend aligns with the increasing kinetic rates of MSW devolatilization at higher temperatures.

Conversely, the yield of pyrolytic oil increased with temperature from 350 °C to 500 °C, reaching a peak of 50 % at 450–500 °C, before declining at 550 °C. Above 500 °C, the thermal cracking of pyrolysis vapors likely leads to the formation of non-condensable gases such as carbon monoxide, hydrogen, carbon dioxide, and light hydrocarbons. This hypothesis is supported by the significant increase in gas yield at 550 °C. While the gas yield remains around 10 % between 350 °C and 500 °C, it rises to approximately 20 % when the MSW is heated to 550 °C.

From an experimental perspective, the material loss was approximately 10 % across all four tests. A visual inspection revealed a tarry, sticky deposit in the cold zones of the tube furnace and within the pipelines, which can undoubtedly be attributed to the condensation of pyrolysis vapors. The formation of such deposits may pose a technological challenge that needs to be addressed.

As previously described, the oil fraction was recovered by quenching in cold water, achieved by bubbling the pyrolysis vapors through three consecutive flasks. However, this method did not allow for efficient oil recovery necessary for proper characterization. Oil recovery remains one of the major technological challenges in a pyrolysis plant. Conventional heat exchanger condensers cannot be used due to rapid and severe fouling of the equipment. Additionally, upon cooling, pyrolysis vapors tend to form aerosols, making effective separation from gases more difficult.

A rapid quenching process is essential to preserve the bio-oil's chemical compounds, preventing further cracking into permanent gases or polymerization into char. Industrially, simple columns or Venturi scrubbers can be employed for oil recovery from pyrolysis vapors. However, oil recovery is just one of several critical challenges in pyrolysis plants.

Pyrolysis oil derived from biomass or municipal solid waste (MSW) is a complex mixture containing a wide range of organic compounds, including hydroxyaldehydes, hydroxyketones, sugars, phenols, and carboxylic acids. These compounds significantly alter the physicochemical properties of the oil during storage. In particular, bio-oil aging is primarily characterized by a substantial increase in viscosity due to polymerization reactions, leading to the formation of a multiphase system composed of tars, sludge, waxes, and aqueous phases.

Furthermore, MSW-derived bio-oil exhibits a broad range of properties and compositions, depending on the pyrolysis technology, process conditions, and feedstock characteristics. However, some common features of pyrolysis oils have been identified in the literature: they are highly acidic (pH 2–4), contain a high water content (15–30 wt%), have a moderate heating value (15–24 MJ/kg), and possess very low ash content (0.05–0.1 wt%) [50].

The organic phase of pyrolysis oil has the potential to be upgraded for use as a fuel in heat and power generation. However, significant technical challenges remain. Unlike crude oil, bio-oil cannot be fractionated by conventional distillation. Upon heating, both light volatiles and water evaporate, while the remaining fraction undergoes polymerization, forming a residual solid phase. Over the past few decades, various bio-oil upgrading techniques have been proposed, including hydrotreating, hydrocracking, supercritical fluid extraction, solvent addition, esterification, emulsification, and steam reforming. Despite their potential, none of these technologies have been commercialized due to technical limitations and high costs. Consequently, bio-oil upgrading remains one of the major drawbacks of pyrolysis plants.

Currently, pyrolysis oil is primarily used as a low-quality, low-value fuel for heat production, but it presents several challenges in terms of

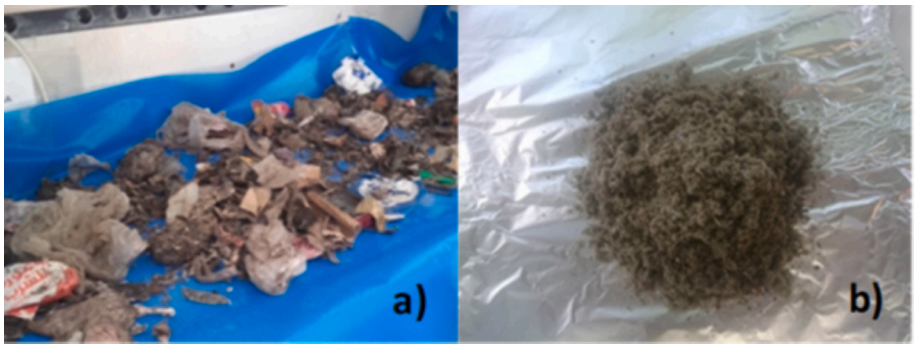

Fig. 6. a) The municipal solid waste (as received); b) Milled MSW inert free.

Table 3
Chemical physical analysis of MSW.

Proximate analysis			
	MSW as received	MSW inert free	Method
Moisture, wt%	45		modified UNI EN 15414
Fix carbon, wt% dry	3.4*	4.0 + 0.3	UNI EN 15148
Ash, wt% dry	35.3*	24.40 + 2.32	UNI EN 14775
Volatiles, wt% dry	61.3*	71.6 + 0.3	UNI EN 15148
Elemental analysis			
C, wt% dry		29.79	
H, wt% dry		5.46	
N, wt% dry		1.35	
S, wt% dry		0.13 + 0.01	
F, wt% dry		0.0049 + 0.0003	ISO 16948
Cl, wt% dry		0.91 + 0.01	
Br, wt% dry		Not detected	
P, wt% dry		Not detected	
O, wt% dry		38.0	
Heating value			
HHV, MJ/kgdry	16.2*	18.9 + 0.2	UNI EN 14918
LHV, MJ/kgdry	–	17.8 + 0.2	

* Calculated from the experimental measure of MSW inert free.

Table 4
Metal concentration (expressed in mg/kg) in inert free MSW.

Al	Co	Cr	Cu	Mn	Mo
4267.2 (224.1)	2.1 (0.2)	52.9 (4.4)	32.6 (0.5)	139.9 (9.4)	2.8 (0.3)
Tl	**V**	**Zn**	**Ca**	**K**	**Mg**
3.1 (0.1)	7.4 (1.2)	84.7 (5.8)	30,602.0 (3710.1)	9500.1 (805.2)	1873.5 (138.0)
Ni	**Pb**	**Ti**	**Na**	**Si**	**Fe**
9.1 (2.1)	61.7 (3.9)	298.3 (37.0)	10,951.6 (491.9)	15,095.0 (1183.1)	31,848.8 (2340.8)

efficiency, operability, cost, and safety [51]. As a result, bio-oil is often burned within the pyrolysis plant itself to sustain the process. Although exploring alternative strategies for the sustainable valorization of bio-oil is crucial, this topic falls beyond the scope of the present study. Therefore, the produced bio-oil was not extensively characterized, and only its yield was reported.

In contrast, the solid residue from pyrolysis, known as bio-char (pyro-char), is commonly utilized as an alternative to charcoal for producing high-value products such as carbon black and activated carbons. Additionally, bio-char can serve as a soil amendment, enhancing soil properties by retaining water, nutrients, and agricultural chemicals, thereby preventing groundwater contamination and soil erosion. The application of bio-char in agriculture also aids in carbon sequestration,

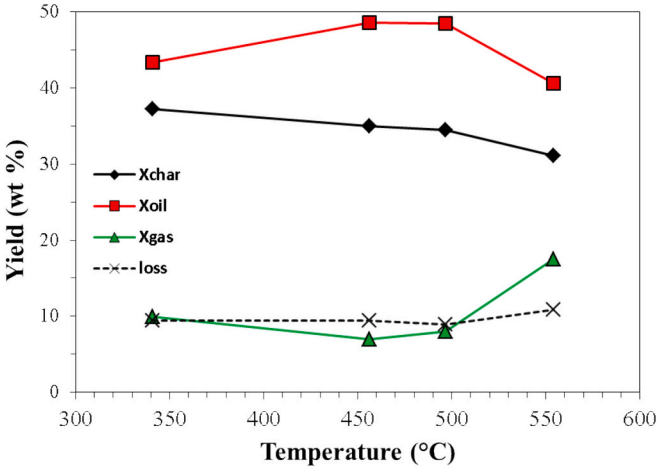

Fig. 7. Product distribution as a function of pyrolysis temperature.

contributing to a reduced carbon footprint [52].

The pyro-char obtained from pyrolysis tests at different temperatures was characterized through proximate and elemental analyses, with the key results presented in Table 5. The notation CharT is used to indicate the average pyrolysis temperature T at which the municipal solid waste was processed.

It is particularly noteworthy that the ash content in the char increases with pyrolysis temperature. This experimental observation supports the progression of MSW pyrolysis as the temperature rises.

Regarding the heating value, a decreasing trend was observed with increasing pyrolysis temperature. This decline is directly linked to the increasing ash content and the decreasing organic fraction at higher temperatures.

The elemental composition of the char exhibits a non-monotonic trend for each element (C, H, N, O) as the pyrolysis temperature changes. Understanding this behavior is challenging and is likely due to

Table 5
Char proximate analysis and heating value.

Proximate analysis wt%					
	Char341	Char456	Char496	Char554	MSW
volatile	28.8	22.8	20.6	15.8	71.6
ash	50.2	54.6	54.6	62.7	24.40
fixed Carbon	21.0	22.6	24.8	21.5	4.0
Elemental analysis wt%					
C	13.69	9.54	15.52	14.67	29.79
H	2.61	1.86	4.41	2.52	5.46
N	0.66	0.56	0.84	1.04	1.35
O	32.8	33.4	24.6	19.07	38.0
LHV MJ/kg	13.4	12.1	10.8	10.6	17.8

the complex physicochemical phenomena governing the pyrolysis process. However, some insightful conclusions can be drawn by comparing the elemental composition of the chars with that of the original MSW. The carbon content in char is approximately half or less than that of MSW at all pyrolysis temperatures.

The oxygen content decreases to about half of its initial value in MSW when the pyrolysis temperature reaches 550 °C. This suggests that dehydrocarbonization primarily occurs at lower pyrolysis temperatures, while at temperatures above 500 °C, dehydroxycarbonization becomes more pronounced.

Several studies in the literature have identified various chemical mechanisms governing devolatilization through thermal analysis. However, due to the heterogeneous nature of MSW, its components may interact with one another during degradation. As a result, defining the precise decomposition temperature range for each component and explaining their individual degradation mechanisms remains challenging.

Fig. 8 presents the average composition of pyrolysis gas (pyro-gas) as a function of process temperature.

The primary compounds detected in the pyrolysis gas stream are CO, CH_4, CO_2, H_2, and light hydrocarbons (mainly C_2–C_3). The product distribution is strongly influenced by process temperature. Carbon monoxide is the most abundant component (approximately 40 %) across the entire temperature range, followed by methane (20–25 %).

A clear increasing trend is observed for both hydrogen content and the total fraction of hydrocarbon molecules. Specifically, hydrogen content rises from 10 % to 15 % as the temperature increases from 341 °C to 554 °C, while the total hydrocarbon content (including methane, ethane, ethylene, and propane) increases from 36 % to 41 %. Conversely, carbon dioxide concentration decreases significantly with increasing temperature, dropping from 15 % at 341 °C to 7 % at 554 °C. The formation of CO_2 is typically associated with decomposition carboxyl groups, which occur at relatively low temperatures [53,54]. At higher temperatures, secondary reactions of volatiles predominantly produce CH_4 and CO rather than CO_2, leading to a reduction in CO_2 content.

The concentrations of ethane and ethylene appear largely unaffected by temperature, while a slight increase in propylene production is observed at higher temperatures.

Similar results have been reported in literature. Fu et al. associate the reduction of CO_2 with the temperature mainly to the cracking and reforming of carboxyl groups, while secondary reactions of volatiles at higher temperature cause the generation of CO and CH_4 [55]. Gao et al. with a study on the pyrolysis of sewage sludge claim that higher concentrations of H_2, CH_4, and CO, at higher temperature could be related to the occurring of secondary thermal decomposition reactions of the primary volatiles that are favoured at higher temperature. The authors also observed the reduction of CO_2 at higher temperature that could be also related to secondary reaction of bio-oil and further formation of char via polymerization [56]. The decreasing of CO_2 concentration could be then related to Boudouard reaction that is favoured at higher temperature, where CO_2 can be consumed through reaction with solid carbon forming CO [57].

The lower heating value (LHV) of pyrolysis gases increases from 23.7 MJ/kg to 34.2 MJ/kg as the temperature rises from 341 °C to 496 °C. At 554 °C, the LHV slightly decreases to 33.7 MJ/kg. Nevertheless, the obtained values suggest that pyro-gas is a viable energy source for heat production, either within the pyrolysis process itself or for power generation. Additionally, pyro-gas can be further upgraded to achieve a composition suitable for chemical production, as will be discussed later.

3.3. Gasification tests of pyro-char

Both the high ash content and the low heating value of the obtained pyro-char (see Table 5) limit its suitability as a solid recovered fuel for heat production [58]. However, the residual carbon can be further valorized and converted into higher-value products, such as syngas.

To both reduce and utilize the pyro-char, gasification tests were conducted under air flow, following the procedure outlined in the Experimental section.

Fig. 9 illustrates the raw gas composition as a function of time (light hydrocarbons, such as C2-C3, lower than 0.1 %). At time zero, when the char is introduced into the kiln, it undergoes combustion due to the presence of a highly oxygen-rich environment. As a result, the molar concentration of CO_2 increases while the oxygen content decreases.

A steady-state condition is reached after approximately 40 min, at which point the gas composition stabilizes. The raw gas contains a relatively high nitrogen concentration (approximately 60 mol%), resulting in a low heating value of about 3.8 MJ/Nm^3.

At steady state, the primary gasification products are carbon monoxide (approximately 20 mol%), hydrogen (approximately 10 mol%), and carbon dioxide (approximately 10 mol%), with trace amounts of methane and light hydrocarbons (<1 %). The total volume of produced gas was 1.4 Nm^3 per kg of char, with an average char conversion of 60 %.

The gas obtained from gasification can be utilized for: (i) energy production (heat and power) or (ii) chemical synthesis.

For energy applications, properly purified gasification gas can be used in gas engines, turbines, or fuel cells for power generation. Internal combustion gas engines are commonly employed in relatively small-scale plants (up to 10 MW) due to their lower capital and maintenance costs. However, a major challenge in commercializing biomass-based combined heat and power (CHP) systems is the presence of tars and particulates in the gas. These contaminants cause damage to process equipment and engines, significantly increasing maintenance costs.

Similar challenges arise when syngas is used in chemical synthesis, such as hydrogen, methanol, olefins, or Fischer-Tropsch fuels via conventional catalytic processes. In these cases, the presence of tars, particulates, and sulfur- or nitrogen-containing compounds must be minimized to prevent catalyst deactivation. Various syngas cleaning strategies can be implemented to address these issue [59].

The raw gas produced from char gasification contained approximately 0.95 g/Nm^3 (dry gas) of gravimetric tar and 0.28 g/Nm^3 (dry gas) of particulates. These values are quite promising, considering that

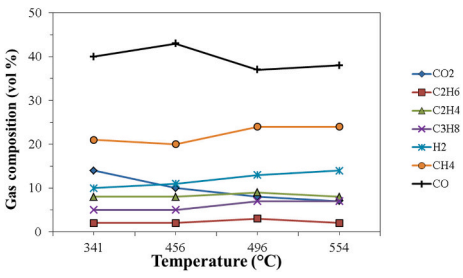

Fig. 8. Pyrolysis gas composition as function of the average process temperature.

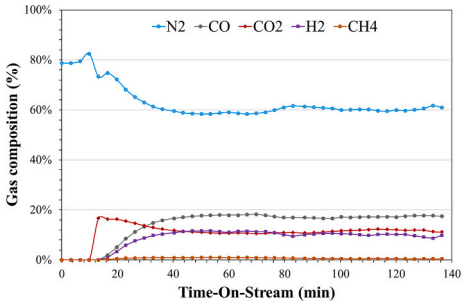

Fig. 9. Producer gas molar composition from char gasification.

commercial technologies for tar and particulate removal—such as cyclones, barrier filters, high temperature treatments, wet electrostatic precipitators (ESPs), and wet scrubbers—typically achieve removal efficiencies above 90 % [60,61].

The low tar concentration is primarily attributed to the fact that the char used as feedstock for the gasifier was obtained through pyrolysis, a process in which most of the MSW volatiles were already vaporized (as evidenced by the volatile content in Table 4). These volatile compounds include alcohols, ketones, aldehydes, and carboxylic acids, collectively referred to as primary tars [62,63].

In addition, organic contaminants were analyzed using GC–MS techniques. The identified aromatic compounds included pyridine, naphthalene, phenanthrene, fluoranthene, and pyrene, with their relative abundances shown in Fig. 10.

The most abundant molecule is naphthalene (50 wt%), followed by pyrene (21 wt%) and fluoranthene (16 wt%). Naphthalene is thermodynamically a very stable tar component, primarily formed from phenolic molecules in the primary tar [64]. The relative distribution of tar molecules aligns with the findings of several researchers who identified naphthalene and non-substituted polycyclic aromatic hydrocarbons (PAHs) as the most abundant molecules [65,66].

The concentration of chromatographic tar in the raw gas was 1.74 g/Nm^3 dry gas. The discrepancy between the chromatographic and gravimetric data is attributed to the experimental procedure used for the gravimetric tar measurement. It is likely that, during the evaporation of the ethanol solution containing the tar, lighter molecules with higher vapor pressure, such as naphthalene and phenanthrene, were partially volatilized [67].

3.4. Process simulation for gas stream valorisation

As previously mentioned, the valorization of both pyrolysis and gasification gas streams was evaluated by simulating the production of electricity, methanol, or pure hydrogen. The gas composition was based on experimental observations. Specifically, for the pyrolysis step, data collected at 456 °C were used to maximize the CO concentration in the gas stream. The gas composition and key parameters used in the simulation are reported in Table 6 and Table 7, respectively. A plant size of 100,000 t/y of MSW was considered as the medium size for an MSW treatment plant.

Table 8 presents the process results for the three cases considered. HTS-WGS and LTS-WGS conversions were 45 % and 37 %, respectively. HTS-WGS conditions are favorable due to the higher CO concentration, while LTS-WGS conditions are thermodynamically optimal due to the lower temperature, though the reactant concentration is lower than in the HTS-WGS reactor. To achieve a $(H_2\text{-}CO_2)/(CO + CO_2)$ ratio of 2, an 87 % carbon capture section was required. As a result, a rich-CO_2 syngas at 35 bar was obtained. The same results were observed for the Case-H2.

The total carbon $(CO + CO_2)$ conversion in the MeOH reactor was 56 %. This corresponds to a 12 % conversion considering a single pass through the MeOH reactor. A purge split ratio of 10 % was set to maintain a $(H_2\text{-}CO_2)/(CO + CO_2)$ ratio of 2 at the reactor inlet.

In the PSA process, an 85 % hydrogen recovery was achieved, with an inlet pressure of 35 bar. The chemical yields were approximately 4 % (3732 t/y) for methanol and about 1 % (1000 t/y) for pure hydrogen.

The reported yields are calculated considering the "unsorted" MSW, including moisture, ash and inerts of the feedstock. By considering the elemental analysis of the sample, the hydrogen and carbon flowrates with the feedstock are around 2500 t/y and around 13,400 t/y, respectively, indicating a yield equals to 40 % on hydrogen basis for the hydrogen production, and 10 % on carbon basis for methanol production. These values are lower than those usually obtained through gasification of lignocellulosic biomasses, especially for methanol production. For instance, Kumabe et al. obtained a methanol yield in the range 30.9–47.7 % by steam gasification of wood, and similar results were obtained with oxygen-steam gasification of Solid Recovered Fuel and Lignite mixture, or Refuse Derived Fuel (RDF) [68–70]. Higher hydrogen yields were obtained for biomass gasification, but in the case of gasification of waste, similar results are obtained, especially with air as gasifying agent [71–73]. Higher hydrogen yields are obtained if steam is as gasifying agent [74]. In the present study, the high ash content of the feedstock, the internal energy use, i.e. combustion of bio-oil, and relatively low C conversion efficiency due to syngas dilution with nitrogen, are the main causes of low yields. On the other hand, the utilization of a nitrogen-free gasification, like oxygen-steam gasification, or the direct gasification of the MSW would reasonably increase the complexity of the concept, from a technical and process point of view. Following the adopted approach, a simpler route for the waste valorization is obtained with benefits from an environmental point of view, as

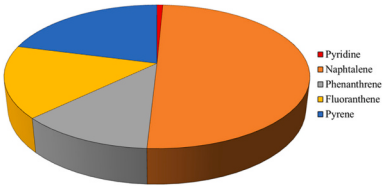

Fig. 10. Relative distribution of tar from GCMS analysis.

Table 6
Pyrogas and gasification syngas compositions (%$_{voldry}$).

	Pyrogas	Syngas
CO_2	10	11.0
C_2H_6	2	0.2
C_2H_4	8	0.0
C_3H_8	5	0.0
H_2	11	11.1
CH_4	20	0.9
CO	43	17.2
N_2	0	59.6

Table 7
Process simulation parameters.

	EL	MeOH	H_2
MSW flowrate (t/y)	100′000		
Pyrogas yield (t/t_{MSW})	0.07		
Biochar yield (t/t_{MSW})	0.35		
Bio-oil yield (t/t_{MSW})	0.58		
MeOH reactor pressure (bar)	–	80	–
CO2 captured pressure (bar) [39]	–	110	110
DEPG/CO2-rich syngas ratio (mol/mol) [31]	–	2.8	2.8
MeOH purification columns pressure (bar)	–	2	–
Steam to CO ratio in WGS (mol/mol) [39]	–	2.5	2.5
Pyrolisys temperature (°C)	456		
Gasification temperature (°C)	800		
Selexol separation temperature (°C)	–	35	35

Table 8
Process simulation main results.

	EL	MeOH	H2
CO_2 captured by Selexol® (%)	–	87	87
Engine inlet pressure	35	80	97
Selexol® separation pressure (bar)	35	35	35
CO_2 captured by Selexol® (kt/y)	0	22.5	22.5
CO conversion in HT-WGS reactor (%mol)	–	45	45
CO conversion in LT-WGS reactor (%mol)	–	37	37
Global CO + CO_2 conversion to MeOH (%mol)	–	56	–
Pure hydrogen recovery in PSA (%)	–	–	85
Pure hydrogen production (kt/y)	–	–	1.0
Methanol production (kt/y)		3.7	
GEn (GJ/y)	95′386	94′784	137′117

also described below.

Similarly,

The global energy of the products is calculated as follows:

$$GEn = 3.6\,\boldsymbol{P} + 0.12\,\dot{\boldsymbol{n}}_{H_2} + 0.0197\,\dot{\boldsymbol{n}}_{MeOH}$$

Where *GEn* represents the global energy produced in the year (GJ/y), $\boldsymbol{P}$ is the green power produced for the investigate case and $\dot{\boldsymbol{n}}_{H_2}$ and $\dot{\boldsymbol{n}}_{MeOH}$ are the hydrogen and methanol production rate, respectively.

As reported in Table 8, the global energy is higher for the Case-H2 due to the higher LHV of pure hydrogen.

Electricity production in the EL case was 3.68 MWe, i.e. around 300 kWhe/ton_{MSW}. Higher values are obtained in the case of incineration of higher quality waste, i.e. Solid Recovered Fuel (SRF), also considering internal energy consumption [75]. In respect to conventional incineration, the proposed two-step scheme, i.e. pyrolysis followed by gasification, causes a loss of stream as bio-oil, that is used as fuel for supporting the pyrolysis unit. However, while the electricity yield might be lower than direct incineration in some cases, pyro-gasification offers potential advantages such as the production of higher-value chemical feedstocks (methanol, hydrogen) and the possibility of more efficient CO_2 capture integration and avoid ash melting due to the lower temperature [76,77].

In the MeOH case, the combustion of purge gas generated a gross power output of 4.05 MWe. However, power consumption for carbon capture (−2.31 MWe), the methanol reactor (−0.86 MWe), and gas recycling (−0.06 MWe) reduced the gross power to a net output of 0.82 MWe.

In the H_2 case, only the power required for carbon capture was considered. Here, the combustion of purge gas resulted in a gross power output of 2.96 MWe.

For both the MeOH and H_2 cases, the compression of captured CO_2 was also taken into account, requiring an additional 0.31 MWe of electrical power.

The net power outputs for all cases are summarized in Fig. 11.

The annual CO_2 equivalent emissions are presented in Fig. 12. Direct emissions include those from the combustion of bio-oil, CO_2 captured in the Selexol® process (if it is not compressed and stored), and the flue gases generated from the combustion of syngas or purge gas.

Indirect emissions include the disposal of solid char residue post-gasification and process water from the Water-Gas Shift (WGS) reaction. The orange bars in the figures represent savings achieved by avoiding landfilling of Municipal Solid Waste (MSW).

The largest emission source is the combustion of bio-oil, which supports the pyrolysis reaction. Approximately 25 % of these emissions are attributed to solid residue disposal. Direct emissions from syngas combustion significantly exceed those from purge gas combustion, reflecting the greater amount of combustible material involved. The

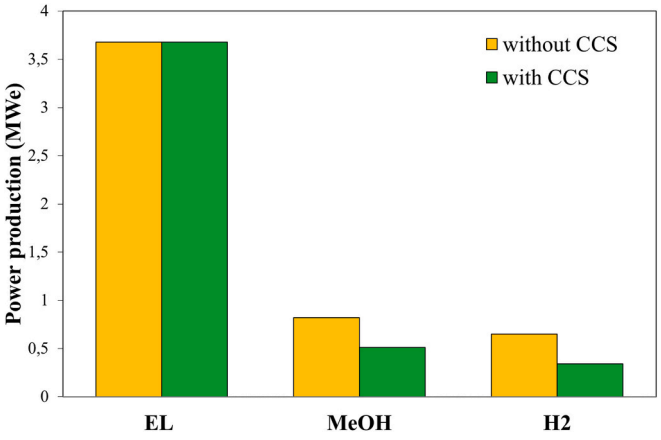

Fig. 11. Electric power production for EL, MeOH, and H2 cases. Calculation base: 100 kt/y of MSW.

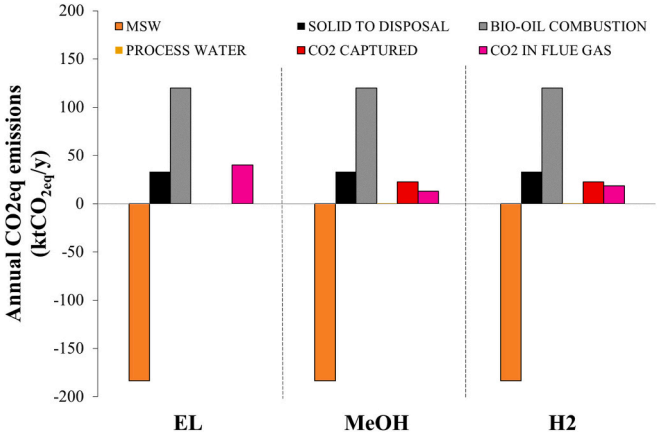

Fig. 12. Annual CO_2 equivalent emissions for EL, MeOH and H2 cases. Savings from MSW (orange bars), emissions from solid residual after gasification (black bars), bio-oil combustion (gray bars), process water (yellow bars), CO_2 captured in Selexol process (red bars), combustion of syngas/purge gas (rose bars). Calculation base: 100 kt/y of MSW. (For interpretation of the references to color in this figure legend, the reader is referred to the web version of this article.)

captured CO2 is roughly equivalent to the difference between the flue gas emissions in the Electricity (EL) case and the emissions from purge gas combustion (for Methanol (MeOH) and Hydrogen (H2) production).

Fig. 13 illustrates the total emissions from Fig. 12, categorized as "Emissions and MSW savings."

Without CO_2 storage, Case-H2 exhibits the highest emissions, while MeOH shows the lowest. This is due to the high emissions in Case-H2, resulting from purge gas combustion. In Case-H2, green power production is reduced as the hydrogen's calorific value is diverted from the Pressure Swing Adsorption (PSA) process, and the CO_2 is released into the atmosphere via the purge gas flue.

With CO_2 storage (Fig. 13, left), both MeOH and H_2 cases show negative values, indicating that the savings from utilizing MSW instead of landfilling outweigh direct and indirect emissions. In this scenario, the MeOH case demonstrates a greater overall saving. Fig. 13 also presents savings from MeOH and pure H_2 products ("Product savings") and green power production. The total savings (product + electricity) are highest in the EL case and lowest in the MeOH case. This is attributed to the higher green power savings in the EL case compared to the combined product and green power savings in the other cases. This disparity stems from the low overall yields of MeOH and pure H_2, at 4 % and 1 %, respectively. Chemical production reduces electricity output but yields limited product quantities.

CO_2 storage significantly impacts CO_2 emissions, as evident from Fig. 13. Without storage, the EL case achieves the highest savings, while Case-H2 shows the lowest. This is due to the low product savings in the MeOH and H2 cases and the high emissions from purge gas combustion in Case-H2. In Case-H2, green power production is reduced due to the hydrogen's calorific value being diverted from PSA, with the CO_2 released in the purge gas fumes. Conversely, in the MeOH case, the post-capture residual CO_2 is partially converted into MeOH.

With CO_2 storage, the highest savings are observed for MeOH and H_2 (nearly identical), and the lowest for EL. This occurs because the 22.5 kt/y of captured and stored CO_2 represents 12 % of the total emissions in the MeOH and H_2 cases, and 462 % and 212 % of the net emissions (considering MSW savings) for MeOH and H_2, respectively.

Further studies should be focused on the assessment of char gasification with different gasifying agent, such as oxygen/steam mixture. Indeed, while air gasification is suitable for electricity generation, it could be no advantageous for methanol synthesis, where a high pressure of reactants is requested for synthesis. Indeed, the presence of nitrogen dilutes the gas and higher reaction pressure are requested to obtain the

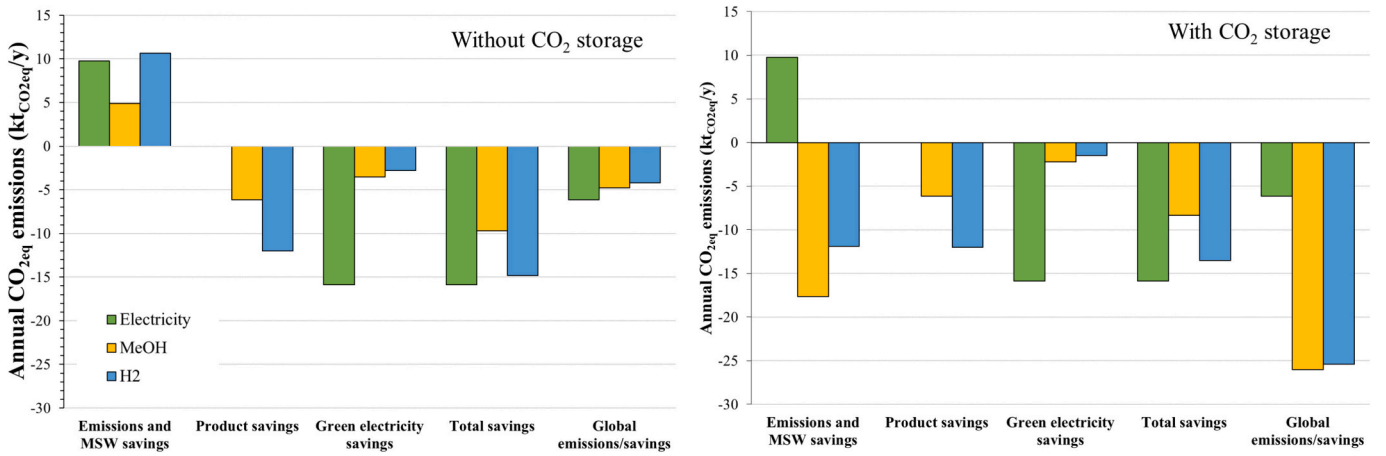

Fig. 13. Annual CO2 equivalent emissions for MSW valorization towards electricity (green bars), methnaol (yellow bars), hydrogen (blue bars), without CO_2 sequestration (left) and with CO_2 sequestration (right). (For interpretation of the references to color in this figure legend, the reader is referred to the web version of this article.)

same methanol yields of nitrogen-free processes. However, alternative gasifying agents like oxygen/steam mixture usually increase the gasification costs due to the needs to produce steam and pure oxygen [78,79]. The utilization of pure oxygen as side-product of green hydrogen production via water electrolysis could be considered for further simulation assessments [80].

Furthermore, albeit no issues related to the high ash content, i.e. slagging, were observed, the management of ash could be a potential issue in full-scale system. At this regard, a good control of temperature during gasification could avoid ash melting in the reactor and additional assessment should be carried out to assess potential application of residual ashes [81,82]. Also other aspects should be addressed in details for full-scale application like chlorine management. The presence of chlorine in the feedstock can indeed create corrosion issues, especially in the units downstream of pyro-gasification unit [83]. Strategies have been developed to address this issue, like hot gas cleaning techniques with inorganic sorbents [55,84,85].

Moreover, in order to assess in more details the reliability of the proposed scheme for the valorization of the investigated MSW, additional studies at pilot scale should be carried out. Investigation at higher scale indeed would allow to consider aspects that can hardly be addressed at lab-scale, like the achievement of autothermal conditions in the gasifier or the real energy demand of the pyrolysis unit, in order to evaluate the scalability of the process [86]. These studies could provide realistic data for a preliminary economic assessment of the plant. Finally, the proposed scheme should be tested with other feedstocks, i.e. plastic waste, residual biomass, digestate and also with other technologies, i.e. catalytic pyrolysis, with the aim to assess their effect on the final product yield and environmental benefits [87–89].

4. Conclusion

This work proposes the valorization of unsorted municipal solid waste (MSW) from Morocco for the production of chemicals (i.e., methanol or hydrogen) and green electrical power, integrating both experimental tests and simulations.

In the experimental part, the pyrolysis of MSW was studied over a wide temperature range (350–550 °C). The resulting pyro-char was then gasified with air to produce syngas and reduce the solid residue. The gas streams produced from both the pyrolysis and gasification units were used as input material streams for simulating the production of methanol, hydrogen, or electric power.

Pyrolysis temperature significantly influences the product distribution. In particular, both the oil and char yields decrease with increasing temperature, favoring gas production, though this trend becomes more pronounced at higher temperatures. The gas yield ranged from about 10 % in the 350–500 °C range, increasing to 20 % at 550 °C. The liquid fraction obtained from pyrolysis (bio-oil) was considered for combustion to support the endothermicity of the pyrolysis reactions. On the other hand, the obtained pyrolysis char was gasified at 800 °C with sub-stoichiometric air, resulting in a syngas mainly containing CO (about 50 vol% N_2-free), H_2 (about 20 vol% N_2-free), and CO_2 (about 20 vol% N_2-free).

Computer-assisted process simulations considered the gas streams produced from both pyrolysis and gasification units as starting materials. After applying the water gas shift and carbon capture processes, calculations indicate that from the obtained syngas, approximately 4000 tons/year of methanol and 1000 tons/year of hydrogen can be produced from 100,000 tons/year of MSW. Additionally, syngas can be used to produce 300 kWh(e)/ton of MSW.

Notably, the production of green electricity results in the highest CO_2 equivalent savings, about 60 t_{CO_2eq}/ktMSW. When CO_2 storage is added to capture, the optimal CO_2eq savings are similar for methanol and pure hydrogen production, with reductions of 48 t_{CO_2eq}/ktMSW and 42 tCO_2eq/kt_{MSW}, respectively.

CRediT authorship contribution statement

Cesare Freda: Writing – review & editing, Investigation, Conceptualization. **Aristide Giuliano:** Writing – review & editing, Methodology, Formal analysis, Conceptualization. **Antonio Villone:** Investigation. **Giacinto Cornacchia:** Supervision, Investigation. **Enrico Catizzone:** Writing – original draft, Formal analysis, Conceptualization.

Declaration of competing interest

The authors declare that they have no known competing financial interests or personal relationships that could have appeared to influence the work reported in this paper.

Data availability

Data will be made available on request.

References

[1] A. Demirbas, Waste management, waste resource facilities and waste conversion processes, Energy Convers. Manag. 52 (2011) 1280–1287, https://doi.org/10.1016/j.enconman.2010.09.025.
[2] M. Migliori, E. Catizzone, G. Giordano, A. Le Pera, M. Sellaro, A. Lista, G. Zanardi, L. Zoia, Pilot plant data assessment in anaerobic digestion of organic fraction of

municipal waste solids, Processes 7 (2019) 54, https://doi.org/10.3390/pr7010054.
[3] M.M. Siddiqi, M.N. Naseer, Y. Abdul Wahab, N.A. Hamizi, I.A. Badruddin, Z. Z. Chowdhury, O. Akbarzadeh, M.R. Johan, T.M.Y. Khan, S. Kamangar, Evaluation of municipal solid wastes based energy potential in urban Pakistan, Processes 7 (2019) 848, https://doi.org/10.3390/pr7110848.
[4] A. Makan, D. Malamis, O. Assobhei, M. Loizidou, M. Mountadar, Multi-criteria decision aid approach for the selection of the best compromise management scheme for the treatment of municipal solid waste in Morocco, Int. J. Environ. Waste Manag. 12 (2013) 300, https://doi.org/10.1504/IJEWM.2013.056197.
[5] F. Karouach, M. Bakraoui, Y. El Gnaoui, N. Lahboubi, H. El Bari, Effect of combined mechanical–ultrasonic pretreatment on mesophilic anaerobic digestion of household organic waste fraction in Morocco, Energy Rep. 6 (2020) 310–314, https://doi.org/10.1016/j.egyr.2019.11.081.
[6] M. Saghir, Y. Naimi, S. Belaaouad, Technologies for converting waste into electrical and thermal energy in Fez city (Morocco), in: 2019 International Conference on Wireless Technologies, Embedded and Intelligent Systems (WITS), IEEE, 2019, pp. 1–6, https://doi.org/10.1109/WITS.2019.8723727.
[7] M. Saghir, Y. Naimi, L. Laasri, M. Tahiri, Energy recovery from municipal solid waste in Oujda city (Morocco), J. Eng. Sci. Technol. Rev. 12 (2019) 137–142, https://doi.org/10.25103/jestr.121.16.
[8] A. Barakat, A. Hilali, M. El Baghdadi, F. Touhami, Landfill site selection with GIS-based multi-criteria evaluation technique. A case study in Béni Mellal-Khouribga Region, Morocco, Environ. Earth Sci. 76 (2017) 413, https://doi.org/10.1007/s12665-017-6757-8.
[9] A. Dahchour, S. El Hajjaji, Management of Solid Waste in Morocco, 2020, pp. 13–33, https://doi.org/10.1007/978-3-030-18350-9_2.
[10] M. Gharfalkar, R. Court, C. Campbell, Z. Ali, G. Hillier, Analysis of waste hierarchy in the European waste directive 2008/98/EC, Waste Manag. 39 (2015) 305–313, https://doi.org/10.1016/j.wasman.2015.02.007.
[11] D. Macrì, E. Catizzone, A. Molino, M. Migliori, Supercritical water gasification of biomass and agro-food residues: energy assessment from modelling approach, Renew, Energy 150 (2020) 624–636, https://doi.org/10.1016/j.renene.2019.12.147.
[12] A. Giuliano, E. Catizzone, D. Barisano, F. Nanna, A. Villone, I. De Bari, G. Cornacchia, G. Braccio, Towards methanol economy: a techno-environmental assessment for a bio-methanol OFMSW/biomass/carbon capture-based integrated plant, Int. J. Heat Technol. 37 (2019) 665–674, https://doi.org/10.18280/ijht.370301.
[13] A. Molino, M. Migliori, A. Blasi, M. Davoli, T. Marino, S. Chianese, E. Catizzone, G. Giordano, Municipal waste leachate conversion via catalytic supercritical water gasification process, Fuel 206 (2017) 155–161, https://doi.org/10.1016/j.fuel.2017.05.091.
[14] G. Hamer, Solid waste treatment and disposal: effects on public health and environmental safety, Biotechnol. Adv. 22 (2003) 71–79, https://doi.org/10.1016/j.biotechadv.2003.08.007.
[15] M. Jahirul, M. Rasul, A. Chowdhury, N. Ashwath, Biofuels production through biomass pyrolysis —a technological review, Energies (Basel) 5 (2012) 4952–5001, https://doi.org/10.3390/en5124952.
[16] L. Makarichi, R. Kan, W. Jutidamrongphan, K. Techato, Suitability of municipal solid waste in African cities for thermochemical waste-to-energy conversion: the case of Harare Metropolitan City, Zimbabwe, Waste Manag. Res. 37 (2019) 83–94, https://doi.org/10.1177/0734242X18804029.
[17] M. He, B. Xiao, S. Liu, Z. Hu, X. Guo, S. Luo, F. Yang, Syngas production from pyrolysis of municipal solid waste (MSW) with dolomite as downstream catalysts, J. Anal. Appl. Pyrolysis 87 (2010) 181–187, https://doi.org/10.1016/j.jaap.2009.11.005.
[18] A.M. Li, X.D. Li, S.Q. Li, Y. Ren, N. Shang, Y. Chi, J.H. Yan, K.F. Cen, Experimental studies on municipal solid waste pyrolysis in a laboratory-scale rotary kiln, Energy 24 (1999) 209–218, https://doi.org/10.1016/S0360-5442(98)00095-4.
[19] S. Luo, B. Xiao, Z. Hu, S. Liu, Y. Guan, L. Cai, Influence of particle size on pyrolysis and gasification performance of municipal solid waste in a fixed bed reactor, Bioresour. Technol. 101 (2010) 6517–6520, https://doi.org/10.1016/j.biortech.2010.03.060.
[20] I.I. Ahmed, A.K. Gupta, Pyrolysis and gasification of food waste: Syngas characteristics and char gasification kinetics, Appl. Energy 87 (2010) 101–108, https://doi.org/10.1016/j.apenergy.2009.08.032.
[21] F. Wang, X. Zeng, Y. Wang, J. Yu, G. Xu, Characterization of coal char gasification with steam in a micro-fluidized bed reaction analyzer, Fuel Process. Technol. 141 (2016) 2–8, https://doi.org/10.1016/j.fuproc.2015.04.025.
[22] C. Guizani, M. Jeguirim, R. Gadiou, F.J. Escudero Sanz, S. Salvador, Biomass char gasification by H2O, CO2 and their mixture: evolution of chemical, textural and structural properties of the chars, Energy 112 (2016) 133–145, https://doi.org/10.1016/j.energy.2016.06.065.
[23] W. Zhu, W. Song, W. Lin, Catalytic gasification of char from co-pyrolysis of coal and biomass, Fuel Process. Technol. 89 (2008) 890–896, https://doi.org/10.1016/j.fuproc.2008.03.001.
[24] Y. Huang, X. Yin, C. Wu, C. Wang, J. Xie, Z. Zhou, L. Ma, H. Li, Effects of metal catalysts on CO2 gasification reactivity of biomass char, Biotechnol. Adv. 27 (2009) 568–572, https://doi.org/10.1016/j.biotechadv.2009.04.013.
[25] S. El Hassani, B.E. Lebrouhi, T. Kousksou, A feasibility study of green hydrogen and E-fuels production from a renewable energy hybrid system in the city of Dakhla, Morocco, Int. J. Hydrog. Energy 73 (2024) 316–330, https://doi.org/10.1016/J.IJHYDENE.2024.05.472.
[26] D. Balaban, J. Lubura Stošić, O. Bera, P. Kojić, Performance analysis of refuse-derived fuel gasification plant with carbon capture and storage for power, heating, and hydrogen production, Environ. Prog. Sustain. Energy 43 (2024) e14472, https://doi.org/10.1002/EP.14472.
[27] P. Sharma, P.N. Sheth, B.N. Mohapatra, Recent progress in refuse derived fuel (RDF) co-processing in cement production: direct firing in Kiln/Calciner vs process integration of RDF gasification, Waste Biomass Valoriz. 13 (2022) 4347–4374, https://doi.org/10.1007/S12649-022-01840-8.
[28] I.B. Adefeso, A.M. Rabiu, D.I. Ikhu-Omoregbe, Refuse-derived fuel gasification for hydrogen production in high temperature proton exchange membrane fuel cell base CHP system, Waste Biomass Valoriz. 6 (2015) 967–974, https://doi.org/10.1007/S12649-015-9415-Y.
[29] C.A. Salman, C.B. Omer, Process modelling and simulation of waste gasification-based flexible polygeneration facilities for power, heat and biofuels production, Energies 13 (2020) 4264, https://doi.org/10.3390/EN13164264.
[30] C. Freda, E. Catizzone, A. Villone, G. Cornacchia, Biomass gasification in rotary kiln integrated with a producer gas thermal cleaning unit: an experimental investigation, Res. Eng. 21 (2024) 101763, https://doi.org/10.1016/j.rineng.2024.101763.
[31] A. Giuliano, M. Poletto, D. Barletta, Process Design of a Multi-Product Lignocellulosic Biorefinery, 2015, pp. 1313–1318, https://doi.org/10.1016/B978-0-444-63577-8.50064-4.
[32] E. Catizzone, Z. Cirelli, A. Aloise, P. Lanzafame, M. Migliori, G. Giordano, Methanol conversion over ZSM-12, ZSM-22 and EU-1 zeolites: from DME to hydrocarbons production, Catal. Today 304 (2018) 39–50, https://doi.org/10.1016/j.cattod.2017.08.037.
[33] G. Bonura, M. Migliori, L. Frusteri, C. Cannilla, E. Catizzone, G. Giordano, F. Frusteri, Acidity control of zeolite functionality on activity and stability of hybrid catalysts during DME production via CO2 hydrogenation, J. CO2 Util. 24 (2018) 398–406, https://doi.org/10.1016/j.jcou.2018.01.028.
[34] E. Catizzone, C. Freda, G. Braccio, F. Frusteri, G. Bonura, Dimethyl ether as circular hydrogen carrier: catalytic aspects of hydrogenation/dehydrogenation steps, J. Energy Chem. 58 (2021) 55–77, https://doi.org/10.1016/j.jechem.2020.09.040.
[35] M.E. Dry, High quality diesel via the Fischer–Tropsch process – a review, J. Chem. Technol. Biotechnol. 77 (2002) 43–50, https://doi.org/10.1002/jctb.527.
[36] E. Ahmad Sonal, S. Upadhyayula, K.K. Pant, Biomass-derived CO2 rich syngas conversion to higher hydrocarbon via Fischer-Tropsch process over Fe–Co bimetallic catalyst, Int. J. Hydrog. Energy 44 (2019) 27741–27748, https://doi.org/10.1016/j.ijhydene.2019.09.015.
[37] W.X. Peng, L.S. Wang, M. Mirzaee, H. Ahmadi, M.J. Esfahani, S. Fremaux, Hydrogen and syngas production by catalytic biomass gasification, Energy Convers. Manag. 135 (2017) 270–273, https://doi.org/10.1016/j.enconman.2016.12.056.
[38] C. Ward, H. Goldstein, R. Maurer, D. Thimsen, B.J. Sheets, R. Hobbs, F. Isgrigg, R. Steiger, D. Revay Madden, A. Porcu, A. Pettinau, Making coal relevant for small scale applications: Modular gasification for syngas/engine CHP applications in challenging environments, Fuel 267 (2020) 117303, https://doi.org/10.1016/j.fuel.2020.117303.
[39] A. Giuliano, M. Poletto, D. Barletta, Pure hydrogen co-production by membrane technology in an IGCC power plant with carbon capture, Int. J. Hydrog. Energy 43 (2018) 19279–19292, https://doi.org/10.1016/j.ijhydene.2018.08.112.
[40] D. Sofia, A. Giuliano, M. Poletto, D. Barletta, Techno-Economic Analysis of Power and Hydrogen Co-Production by an IGCC Plant with CO_2 Capture Based on Membrane Technology, 2015, pp. 1373–1378, https://doi.org/10.1016/B978-0-444-63577-8.50074-7.
[41] A. Giuliano, E. Catizzone, C. Freda, Process simulation and environmental aspects of dimethyl ether production from digestate-derived syngas, Int. J. Environ. Res. Public Health 18 (2021) 807, https://doi.org/10.3390/ijerph18020807.
[42] A. Rodrigues Gurgel da Silva, A. Giuliano, M. Errico, B.-G. Rong, D. Barletta, Economic value and environmental impact analysis of lignocellulosic ethanol production: assessment of different pretreatment processes, Clean Techn. Environ. Policy 21 (2019) 637–654, https://doi.org/10.1007/s10098-018-01663-z.
[43] J. Pérez, J.M. de Andrés, J. Lumbreras, E. Rodríguez, Evaluating carbon footprint of municipal solid waste treatment: methodological proposal and application to a case study, J. Clean. Prod. 205 (2018) 419–431, https://doi.org/10.1016/j.jclepro.2018.09.103.
[44] J. Li, X. Ma, H. Liu, X. Zhang, Life cycle assessment and economic analysis of methanol production from coke oven gas compared with coal and natural gas routes, J. Clean. Prod. 185 (2018) 299–308, https://doi.org/10.1016/j.jclepro.2018.02.100.
[45] K. Bareiß, C. de la Rua, M. Möckl, T. Hamacher, Life cycle assessment of hydrogen from proton exchange membrane water electrolysis in future energy systems, Appl. Energy 237 (2019) 862–872, https://doi.org/10.1016/j.apenergy.2019.01.001.
[46] Q. Zhang, J. Chang, T. Wang, Y. Xu, Review of biomass pyrolysis oil properties and upgrading research, Energy Convers. Manag. 48 (2007) 87–92, https://doi.org/10.1016/j.enconman.2006.05.010.
[47] M. Zevenhoven-Onderwater, R. Backman, B.-J. Skrifvars, M. Hupa, The ash chemistry in fluidised bed gasification of biomass fuels. Part I: predicting the chemistry of melting ashes and ash–bed material interaction, Fuel 80 (2001) 1489–1502, https://doi.org/10.1016/S0016-2361(01)00026-6.
[48] R. Sun, T.M. Ismail, X. Ren, M. Abd El-Salam, Effect of ash content on the combustion process of simulated MSW in the fixed bed, Waste Manag. 48 (2016) 236–249, https://doi.org/10.1016/j.wasman.2015.10.007.
[49] H. Zhou, A. Meng, Y. Long, Q. Li, Y. Zhang, A review of dioxin-related substances during municipal solid waste incineration, Waste Manag. 36 (2015) 106–118, https://doi.org/10.1016/j.wasman.2014.11.011.
[50] S. Czernik, A.V. Bridgwater, Overview of applications of biomass fast pyrolysis oil, Energy Fuel 18 (2004) 590–598, https://doi.org/10.1021/ef034067u.

[51] X. Lian, Y. Xue, Z. Zhao, G. Xu, S. Han, H. Yu, Progress on upgrading methods of bio-oil: a review, Int. J. Energy Res. 41 (2017) 1798–1816, https://doi.org/10.1002/er.3726.
[52] S. Kizito, H. Luo, J. Lu, H. Bah, R. Dong, S. Wu, Role of nutrient-enriched biochar as a soil amendment during maize growth: exploring practical alternatives to recycle agricultural residuals and to reduce chemical fertilizer demand, Sustainability 11 (2019) 3211, https://doi.org/10.3390/su11113211.
[53] K.D. Maher, K.M. Kirkwood, M.R. Gray, D.C. Bressler, Pyrolytic decarboxylation and cracking of stearic acid, Ind. Eng. Chem. Res. 47 (2008) 5328–5336, https://doi.org/10.1021/ie0714551.
[54] J. Li, P. Jia, X. Hu, D. Dong, G. Gao, D. Geng, J. Xiang, Y. Wang, S. Hu, Steam reforming of carboxylic acids for hydrogen generation: effects of aliphatic chain of the acids on their reaction behaviors, Mol. Catal. 450 (2018) 1–13, https://doi.org/10.1016/j.mcat.2018.02.027.
[55] V. Marcantonio, M. Müller, E. Bocci, A review of hot gas cleaning techniques for hydrogen chloride removal from biomass-derived syngas, Energies 14 (2021) 6519, https://doi.org/10.3390/EN14206519.
[56] N. Gao, C. Quan, B. Liu, Z. Li, C. Wu, A. Li, Continuous pyrolysis of sewage sludge in a screw-feeding reactor: products characterization and ecological risk assessment of heavy metals, Energy Fuel 31 (2017) 5063–5072, https://doi.org/10.1021/ACS.ENERGYFUELS.6B03112.
[57] N. Gao, J. Li, B. Qi, A. Li, Y. Duan, Z. Wang, Thermal analysis and products distribution of dried sewage sludge pyrolysis, J. Anal. Appl. Pyrolysis 105 (2014) 43–48, https://doi.org/10.1016/J.JAAP.2013.10.002.
[58] E. Iacovidou, J. Hahladakis, I. Deans, C. Velis, P. Purnell, Technical properties of biomass and solid recovered fuel (SRF) co-fired with coal: impact on multi-dimensional resource recovery value, Waste Manag. 73 (2018) 535–545, https://doi.org/10.1016/j.wasman.2017.07.001.
[59] L. Devi, K.J. Ptasinski, F.J.J.G. Janssen, A review of the primary measures for tar elimination in biomass gasification processes, Biomass Bioenergy 24 (2003) 125–140, https://doi.org/10.1016/S0961-9534(02)00102-2.
[60] E. Catizzone, C. Freda, A. Villone, A. Romanelli, G. Cornacchia, Gasification of olive tree pruning in a rotary kiln reactor integrated with radio frequency plasma torch, Fuel 381 (2025) 133480, https://doi.org/10.1016/j.fuel.2024.133480.
[61] W. Zhang, H. Liu, I. Ul Hai, Y. Neubauer, P. Schröder, H. Oldenburg, A. Seilkopf, A. Kölling, Gas cleaning strategies for biomass gasification product gas, Int. J. Low-Carbon Technol. 7 (2012) 69–74, https://doi.org/10.1093/ijlct/ctr046.
[62] C. Li, K. Suzuki, Tar property, analysis, reforming mechanism and model for biomass gasification—an overview, Renew. Sust. Energ. Rev. 13 (2009) 594–604, https://doi.org/10.1016/j.rser.2008.01.009.
[63] Q. Gu, W. Wu, B. Jin, Z. Zhou, Analyses for synthesis gas from municipal solid waste gasification under medium temperatures, Processes 8 (2020) 84, https://doi.org/10.3390/pr8010084.
[64] Z. Zhang, S. Pang, Experimental investigation of tar formation and producer gas composition in biomass steam gasification in a 100 kW dual fluidised bed gasifier, Renew. Energy 132 (2019) 416–424, https://doi.org/10.1016/j.renene.2018.07.144.
[65] P. Morf, P. Hasler, T. Nussbaumer, Mechanisms and kinetics of homogeneous secondary reactions of tar from continuous pyrolysis of wood chips, Fuel 81 (2002) 843–853, https://doi.org/10.1016/S0016-2361(01)00216-2.
[66] M. Cortazar, J. Alvarez, G. Lopez, M. Amutio, L. Santamaria, J. Bilbao, M. Olazar, Role of temperature on gasification performance and tar composition in a fountain enhanced conical spouted bed reactor, Energy Convers. Manag. 171 (2018) 1589–1597, https://doi.org/10.1016/j.enconman.2018.06.071.
[67] A. Nzihou (Ed.), Handbook on Characterization of Biomass, Biowaste and Related by-Products, Springer International Publishing, Cham, 2020, https://doi.org/10.1007/978-3-030-35020-8.
[68] K. Kumabe, S. Fujimoto, T. Yanagida, M. Ogata, T. Fukuda, A. Yabe, T. Minowa, Environmental and economic analysis of methanol production process via biomass gasification, Fuel 87 (2008) 1422–1427, https://doi.org/10.1016/J.FUEL.2007.06.008.
[69] A. Rolfe, Y. Huang, N. Hewitt, Methanol production from solid recovered fuel and lignite: techno-economic and environmental assessment, Waste Biomass Valoriz. 13 (2022) 3801–3819, https://doi.org/10.1007/S12649-022-01757-2.
[70] G. Iaquaniello, G. Centi, A. Salladini, E. Palo, S. Perathoner, L. Spadaccini, Waste-to-methanol: process and economics assessment, Bioresour. Technol. 243 (2017) 611–619, https://doi.org/10.1016/J.BIORTECH.2017.06.172.
[71] Y. Alouani, D. Saifaoui, A. Alouani, M.A. Alouani, Municipal solid waste gasification to produce hydrogen: integrated simulation model and performance analysis, Int. J. Energy Res. 46 (2022) 20068–20078, https://doi.org/10.1002/ER.8591.
[72] T. Lepage, M. Kammoun, Q. Schmetz, A. Richel, Biomass-to-hydrogen: a review of main routes production, processes evaluation and techno-economical assessment, Biomass Bioenergy 144 (2021) 105920, https://doi.org/10.1016/J.BIOMBIOE.2020.105920.
[73] S.C. Wijayasekera, K. Hewage, O. Siddiqui, P. Hettiaratchi, R. Sadiq, Waste-to-hydrogen technologies: a critical review of techno-economic and socio-environmental sustainability, Int. J. Hydrog. Energy 47 (2022) 5842–5870, https://doi.org/10.1016/J.IJHYDENE.2021.11.226.
[74] Y. Zhang, P. Xu, S. Liang, B. Liu, Y. Shuai, B. Li, Exergy analysis of hydrogen production from steam gasification of biomass: a review, Int. J. Hydrog. Energy 44 (2019) 14290–14302, https://doi.org/10.1016/J.IJHYDENE.2019.02.064.
[75] J. Dong, Y. Tang, A. Nzihou, Y. Chi, E. Weiss-Hortala, M. Ni, Z. Zhou, Comparison of waste-to-energy technologies of gasification and incineration using life cycle assessment: case studies in Finland, France and China, J. Clean. Prod. 203 (2018) 287–300, https://doi.org/10.1016/J.JCLEPRO.2018.08.139.
[76] S. Consonni, F. Viganò, Waste gasification vs. conventional waste-to-energy: a comparative evaluation of two commercial technologies, Waste Manag. 32 (2012) 653–666, https://doi.org/10.1016/J.WASMAN.2011.12.019.
[77] L. Bébar, P. Stehlík, L. Havlen, J. Oral, Analysis of using gasification and incineration for thermal processing of wastes, Appl. Therm. Eng. 25 (2005) 1045–1055, https://doi.org/10.1016/J.APPLTHERMALENG.2004.07.022.
[78] P. Iovane, A. Donatelli, A. Molino, Influence of feeding ratio on steam gasification of palm shells in a rotary kiln pilot plant. Experimental and numerical investigations, Biomass Bioenergy 56 (2013) 423–431, https://doi.org/10.1016/j.biombioe.2013.05.025.
[79] A. Molino, S. Chianese, D. Musmarra, Biomass gasification technology: the state of the art overview, J. Energy Chem. 25 (2016) 10–25, https://doi.org/10.1016/j.jechem.2015.11.005.
[80] R. Aguado, A. Baccioli, A. Liponi, D. Vera, Continuous decentralized hydrogen production through alkaline water electrolysis powered by an oxygen-enriched air integrated biomass gasification combined cycle, Energy Convers. Manag. 289 (2023) 117149, https://doi.org/10.1016/J.ENCONMAN.2023.117149.
[81] J. Qin, Y. Zhang, S. Heberlein, G. Lisak, Y. Yi, Characterization and comparison of gasification and incineration fly ashes generated from municipal solid waste in Singapore, Waste Manag. 146 (2022) 44–52, https://doi.org/10.1016/J.WASMAN.2022.04.041.
[82] A. Ramos, J. Berzosa, J. Espí, F. Clarens, A. Rouboa, Life cycle costing for plasma gasification of municipal solid waste: a socio-economic approach, Energy Convers. Manag. 209 (2020) 112508, https://doi.org/10.1016/J.ENCONMAN.2020.112508.
[83] W. Ma, T. Wenga, F.J. Frandsen, B. Yan, G. Chen, The fate of chlorine during MSW incineration: vaporization, transformation, deposition, corrosion and remedies, Prog. Energy Combust. Sci. 76 (2020) 100789, https://doi.org/10.1016/J.PECS.2019.100789.
[84] Z. Zhou, Y. Chi, Y. Tang, J. Hu, Effect of calcium-based sorbents on the reduction of chlorinated contaminants during municipal solid waste thermal treatment, Waste Manag. Res. 39 (2021) 1480–1488, https://doi.org/10.1177/0734242X21989793.
[85] C. Borgianni, P. De Filippis, F. Pochetti, M. Paolucci, Gasification process of wastes containing PVC, Fuel 81 (2002) 1827–1833, https://doi.org/10.1016/S0016-2361(02)00097-2.
[86] C. Freda, F. Nanna, A. Villone, D. Barisano, S. Brandani, G. Cornacchia, Air gasification of digestate and its co-gasification with residual biomass in a pilot scale rotary kiln, Int. J. Energy Environ. Eng. 10 (2019) 335–346, https://doi.org/10.1007/S40095-019-0310-3.
[87] R. Miandad, M.A. Barakat, A.S. Aburiazaiza, M. Rehan, A.S. Nizami, Catalytic pyrolysis of plastic waste: a review, Process. Saf. Environ. Prot. 102 (2016) 822–838, https://doi.org/10.1016/J.PSEP.2016.06.022.
[88] R. French, S. Czernik, Catalytic pyrolysis of biomass for biofuels production, Fuel Process. Technol. 91 (2010) 25–32, https://doi.org/10.1016/J.FUPROC.2009.08.011.
[89] L. Quesada, M.C. de Hoces, M.A. Martín-Lara, G. Luzón, G. Blázquez, Performance of different catalysts for the in situ cracking of the oil-waxes obtained by the pyrolysis of polyethylene film waste, Sustainability 12 (2020) 5482, https://doi.org/10.3390/SU12135482.